

Microstructure properties of HVOF-sprayed NiCrBSi/WCCo-based composite coatings on AISI 1040 steel

SERKAN ISLAK^{a,*}, SONER BUYTOZ^b

^a*Kastamonu University, Faculty of Engineering and Architecture, Department of Materials Science and Nanotechnology Engineering, 37000, Kastamonu, Turkey*

^b*Firat University, Faculty of Technology, Department of Metallurgy and Materials Engineering, 23100, Elazig, Turkey*

NiCrBSi/WCCo-based composite coatings were produced on the surface of AISI 1040 steel using high velocity oxygen fuel (HVOF) thermal spraying technique. In the coatings produced, the WCCo quantity added to the NiCrBSi was chosen as 10, 30 and 50 wt. % percentages. The coatings were compared in terms of their phase composition, microstructure, and hardness. Phase composition and microstructure of the coatings were characterised using X-ray diffraction and scanning electron microscopy. The results indicated that the as-prepared NiCrBSi/WCCo-based composite coatings were mainly composed of γ -Ni, WC, W₂C, Cr₂₃C₆, Cr₇C₃, CrB₂, CrSi, and Co phases. Microhardness values of coating layer varied according to the addition of the powder. The highest microhardness value of the coating was measured as 1300 HV_{0.2}.

(Received July 16, 2013; accepted November 7, 2013)

Keywords: HVOF, NiCrBSi, WCCo, Microstructure

1. Introduction

Nickel based alloys, especially NiCrBSi alloys, have high bonding strength, perfect corrosion and wear resistances and thus they are widely used in various industrial areas as coating materials via thermal spray methods [1,2]. Boron in the chemical composition of NiCrBSi based coating powder decreases the melting point of the alloy and provides the formation of hard phases. Silicon is added to improve the self-fluxing properties of alloy powder. Chromium provides high resistance against oxidation and high temperature corrosion. Carbon in the alloy develops carbides with high hardness values and thus increases the wear resistance [3-5].

Ni-based coatings are widely used in the improvement of the surface properties of machines and machine components that are exposed to wear and high temperature corrosion such as chemical industry, petroleum industry, glass form industry, hot working punches, fan paddles, heat exchangers, turbines, extruders, pistons, and agricultural machines [6,7]. Sidhu et al., [8] produced NiCrBSi-based coatings on energy conversion system materials via HVOF spraying method and investigated corrosion behaviour of the coatings. It is determined that in molten salt bath at 900 °C environment; NiCrBSi-based coatings improve the corrosion resistance because it increases the oxide density of nickel, silicon, chromium and boron and such coatings are appropriate for energy conversion systems. NiCrBSi-based coatings, which are produced by thermal spraying methods, are also produced as an alternative to the electrolytic chromium coatings. The expensiveness of electrolytic coating method and the

disadvantages such as the safety and health weakness of the chromium coatings that are also produced in the same way have necessitated the formation of chromium coating via different techniques. Compared to the electrolytic coating, harder coatings are produced by thermal spraying methods. The reinforcement of the chromium-rich nanoparticles to the matrix and the formation of hard phases such as Ni₃B (nickel boride) in the coating provide the hardness of the NiCrBSi coatings that are produced by thermal spraying [9-11].

In order to improve the hardness, wear and corrosion performances of Ni-based alloys; ceramic powders such as TiC [12,13], B₄C [14,15], Cr₃C₂ [16], SiC [17], TiN [18], ZrO₂ [19] and Al₂O₃ [20] are added at specific ratios and metal-matrix composite (MMC) coatings are produced. WC-Co based coatings are generally recommended for wear applications under 500°C. At extensive high temperatures, brittle phases that reduce the wear resistance occur. The cobalt in its composition acts as a matrix and provides a toughness property in the coating.

In this study, NiCrBSi/WCCo based composite coatings were produced by HVOF thermal spraying method. The effect of WC-Co on the microstructure and microhardness was experimentally examined. The microstructure and phase compositions of the coatings were determined via scanning electron microscope (SEM), energy dispersive spectrometer (EDS) and X-ray diffraction (XRD) analyses.

2. Experimental studies

High-velocity oxygen fuel (HVOF) spraying method was used in the production of NiCrBSi/WC-12Co based coatings on the surface of AISI 1040 steel. The composition of the NiCrBSi powder was 74.36 % Ni, 4.73 % Si, 3.97 % Fe, 2.76 % B, 13.68 % Cr, and 0.50 % C. The composition of the WC-12Co powder was 82 % W, 12 % Co, and 6 % C. Nickel based powders had spherical particle size of $-53+15\ \mu\text{m}$ and WC-12Co powders had a nearly spherical structure and the average particle size was $-45+15\ \mu\text{m}$. 10%, 30% and 50% WC-Co powder by weight were added to the NiCrBSi powder. Morphology of NiCrBSi and WC-Co powders is present in Fig. 1.

After cleaning the substrate, used in $\text{Ø}20\times 100\ \text{mm}$ sizes, in an acetone solution, it was exposed to sandblasting process with Al_2O_3 sand having a particle size between 24-35 mesh in order for the coating layer to have a better bonding. Coatings were obtained in the TAFAP-5000 spraying system which is designed to burn the kerosene, produced by distilling from oxygen and petroleum (Fig. 2). During the spraying process; the kerosene and oxygen pressures were fixed at 7.5 bar and 12 bar, respectively. The flow rate of the oxygen was adjusted to 940 l/min and the flow rate of kerosene was adjusted to 0.3 l/min. As the carrier gas; nitrogen gas with 3.5 bar pressure and 12 l/min. flow rate was used. In all the coatings; the spraying distance throughout the coating was selected as 380 mm and powder feed quantity was selected as 152 gr/min.

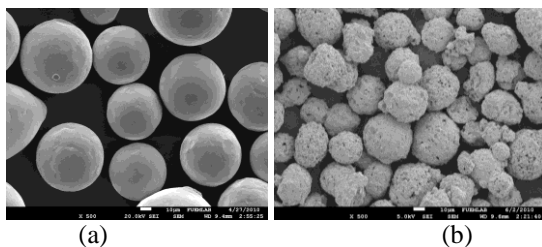


Fig. 1. SEM images of the powders used in the coating process: (a) NiCrBSi and (b) WC-Co.

For metallographic examinations, samples were taken from the section area perpendicular to the coating direction. The metallographic samples obtained were treated with 80-1200 mesh sandpaper and their surfaces were cleaned. Then, side section surfaces were polished by means of 1 and $6\ \mu\text{m}$ diamond paste and diluter. Samples were electrolytically etched in HNO_3 and alcohol mixture solution for microstructural examinations. In each coating, scanning electron microscopy (SEM) and X-ray diffraction (XRD) analyses were used for microstructure and phase analysis. Porosity and average coating thickness were

measured using the image analyzing software. Hardness measurement was performed in loading period of 10 seconds under a load of 200 g using Future-Tech FM 700 brand microhardness device along a line from the top surface of the coating towards the substrate.

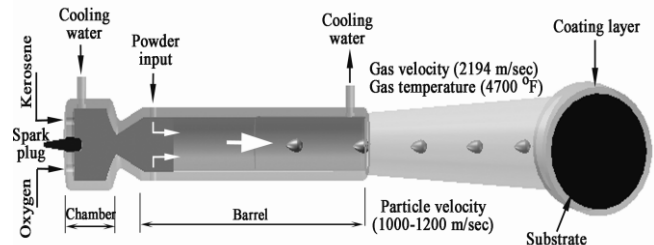


Fig. 2. Principle scheme of HVOF-sprayed process.

3. Results and discussion

Fig. 3 illustrates SEM images of NiCrBSi-WCCo coatings which were fabricated using high velocity oxygen fuel (HVOF) method. The coatings consisted of two zones as coating layer and substrate. A third layer was not formed because the bonding layer powder wasn't used. For the HVOF sprayed NiCrBSi-WCCo coatings, the coating thickness was in the range of 100–150 μm . All coatings were completely crack-free. However, a very small amount of pores in the coatings was observed. The maximum value of porosity, measured along the cross-sectional area using image analyzer software, was found to be less than 1.1%. Amount of pore increased with increasing WCCo content. The WCCo particles were relatively homogeneously distributed in the NiCrBSi matrix. According to the SEM images, there was an increase in the distribution amount of WCCo in the microstructure in parallel with the increase in the mixture rate of WCCo. The bonding between substrate and coating layer seems to be good. Some dark-coloured areas appearing in the coating structure or at the coating-substrate interface may be the inclusions. The SEM images in Fig. 3 illustrate that NiCrBSi particles on the coating layer completely melted at the spraying time. Completely melting of the NiCrBSi particles contributed to the uniformity of the coating [21]. Also from the microstructure images of the coatings; it was understood that the coating layer had a laminar structure. This was caused by re-solidification of molten or semi-molten coating powders [22].

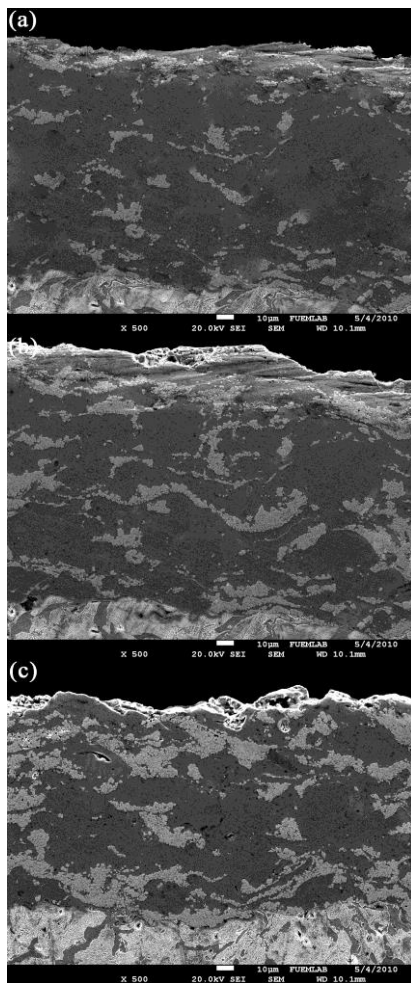


Fig. 3. SEM images of HVOF sprayed NiCrBSi-WCCo coatings: (a) NiCrBSi-10 wt.% WCCo, (b) NiCrBSi-30 wt.% WCCo and (c) NiCrBSi-50 wt.% WCCo.

Fig. 4 illustrates the SEM micrographs showing surface and the EDS analysis at the selected points on the NiCrBSi-50 wt.% WCCo coating. The dark grey area (point 1) contains higher amount of Ni with minor content of Cr, C, B, Fe, Co, Si, and W. Results of this analysis showed that WC grains dissolved partially. The light grey area (point 2) indicates higher amount of W and Co. Point 2 represents WC-Co splats. WC-Co particles striking to the substrate were oriented parallel to the substrate.

Fig. 5 illustrates the XRD graph of NiCrBSi-WCCo coatings produced using HVOF. γ -Ni, WC, W_2C , $Cr_{23}C_6$, Cr_7C_3 , CrB_2 , CrSi, and Co phases formed in the coatings. Principal phases in the coatings were γ -Ni and WC. WC phase transformed to W_2C during spraying. The formation of W_2C phase was regarded as a product of decarburisation in the thermal spraying [22]. As addition quantity of WCCo increased, the intensity of W_2C peak increased. The hard carbides such as $Cr_{23}C_6$ and Cr_7C_3 were formed in the coatings because coating powders contained sufficient amount of Cr and C. The reason behind why Ni-B based compounds did not form or formed in small quantity in the coatings is that Cr quantity

exceeded 8% and B was susceptible to form a compound with Cr. Therefore, CrB_2 phase formed.

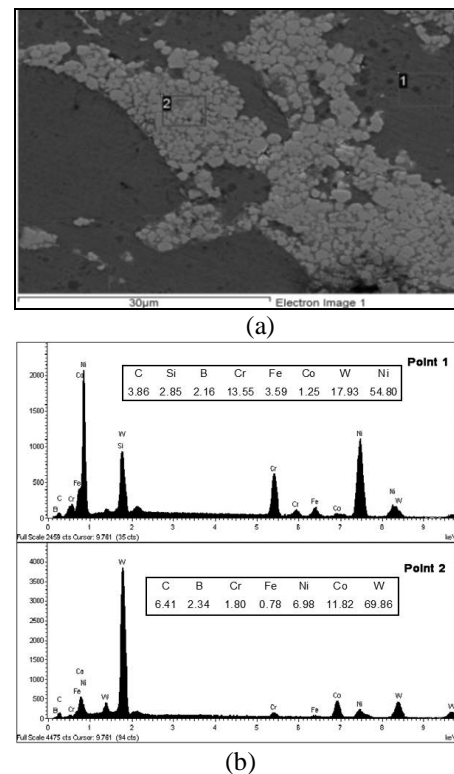


Fig. 4. (a) SEM image and EDS results of NiCrBSi-50 wt.% WCCo coating (b) point 1 and point 2.

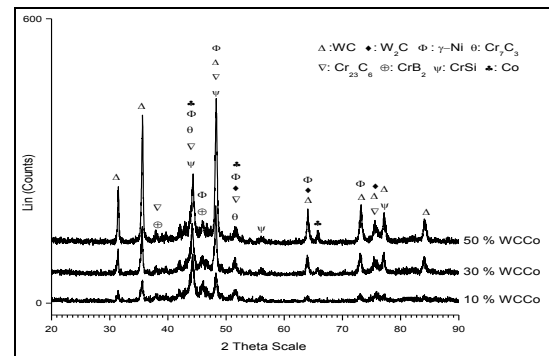


Fig. 5. XRD graph of NiCrBSi-WCCo coatings.

Fig. 6 illustrates the microhardness profile along the depth of the cross-section in the NiCrBSi-WCCo coatings. The microhardness of the substrate was in the range of 350–400 $HV_{0.2}$. The microhardness of the coatings was variable depending on the distance from the coating–substrate interface. The increase in hardness was observed based on the increase in the addition of WCCo powder. The measured average microhardness of NiCrBSi-10 WCCo, NiCrBSi-30 WCCo and NiCrBSi-50 WCCo coatings were 908 $HV_{0.2}$, 1115 $HV_{0.2}$, and 1300 $HV_{0.2}$ respectively. A 2.5–3.5 times increase was determined in the hardness values of the coatings compared to the

substrate. This significant increase in the microhardness of the coatings might be associated with to the distribution of the hard phases such as WC, W_2C , Cr_3C_7 and $Cr_{23}C_6$ in Ni-based matrix. Furthermore, a significant increase in the microhardness values (400-500 $HV_{0.2}$) was measured on the substrate region closer to the coating. This increased hardness might be partially due to both the high speed impact of the coating particles during the HVOF projection and the work hardening effect of the sandblasting of the substrate prior to the coating process [23,24].

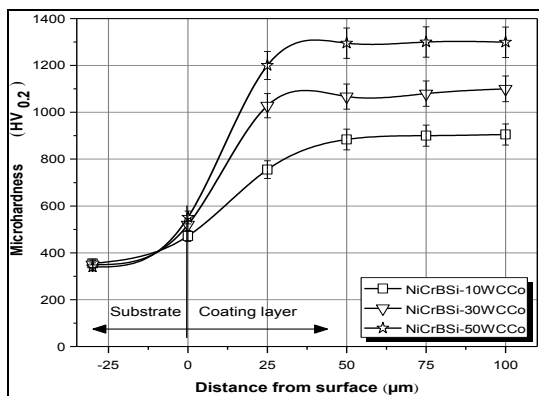


Fig. 6. Microhardness profile of NiCrBSi-WCCo coatings.

4. Conclusions

NiCrBSi-WCCo coatings were successfully produced using HVOF method on AISI 1040 steel. It was understood from SEM images that the WC-Co particles had a relatively homogeneous distribution in the NiCrBSi matrix. NiCrBSi particles on the coating layer completely melted at the during of spraying. Also from the microstructure images of the coatings, it was understood that the coating layer had a laminar structure. XRD analysis results indicated that the NiCrBSi/WC-Co coatings were mainly composed of γ -Ni, WC, W_2C , $Cr_{23}C_6$, Cr_7C_3 , CrB_2 , CrSi, and Co phases. A 2.5-3.5 times increase was determined in the hardness values of the coatings compared to the substrate. The highest hardness value was measured as 1300 $HV_{0.2}$ in coatings produced with 50 % WC-Co addition.

References

- [1] J. Rodriguez, A. Martin, R. Fernandez, J. E. Fernandez, *Wear* **255**, 950 (2003).
- [2] W. M. Zhao, Y. Wang, T. Han, K. Y. Wu, J. Xue, *Surface and Coatings Technology* **183**, 118 (2004).
- [3] M. J. Tobar, C. Alvarez, J. M. Amado, G. Rodriguez, A. Yanez, *Surface and Coatings Technology* **200**, 6313 (2006).
- [4] R. Gonzalez, M. Cadenas, R. Fernandez, J. L. Cortizo, E. Rodriguez, *Wear* **262**, 301 (2007).
- [5] N. Y. Sari, M. Yilmaz, *Surface and Coatings Technology* **202**, 3136 (2008).
- [6] J. M. Miguel, J. M. Guilemany, S. Vizcaino, *Tribology International* **36**, 181 (2003).
- [7] C. Navas, R. Colaco, J. Damborenea, R. Vilar, *Surface and Coatings Technology* **200**, 6854 (2006).
- [8] T. S. Sidhu, S. Prakash, R. D. Agrawal, *Acta Materialia* **54**, 773 (2006).
- [9] S. Abdi, S. Lebaili, *Physics Procedia* **2**, 1005 (2009).
- [10] N. Serres, F. Hlawka, S. Costil, C. Langlade, F. Machi, A. Cornet, *Surface and Coatings Technology* **204**, 197 (2009).
- [11] N. L. Parthasarathi, M. Duraiselvam, *Journal of Alloys and Compounds* **505**, 824 (2010).
- [12] R. L. Sun, D. Z. Yang, L. X. Guo, S. L. Dong, *Surface and Coatings Technology* **135**, 307 (2001).
- [13] Y. Lei, R. Sun, J. Lei, Y. Tang, W. Niu, *Optics and Lasers in Engineering* **48**, 899 (2010).
- [14] Q. W. Meng, L. Geng, B. Y. Zhang, *Surface and Coatings Technology* **200**, 4923 (2006).
- [15] M. Chao, X. Niu, B. Yuan, E. J. Liang, D. S. Wang, *Surface and Coatings Technology* **201**, 1102 (2006).
- [16] Z. Dawei, T. Li, T. C. Lei, *Surface and Coatings Technology* **110**, 81 (1998).
- [17] T. M. Yue, A. H. Wang, H. C. Man, *Scripta Materialia* **40**, 303 (1999).
- [18] R. X. Liu, L. X. Guo, T. Q. Lei, *Surface Review and Letters* **11**, 497 (2004).
- [19] J. H. Ouyang, S. Nowotny, A. Richter, E. Beyer, *Surface and Coatings Technology* **137**, 12 (2001).
- [20] H. Wang, D. Zou, Y. Sun, F. Xu, D. Zhang, *Transactions of Nonferrous Metals Society of China* **19**, 586 (2009).
- [21] T. S. Sidhu, S. Prakash, R. D. Agrawal, *Thin Solid Films* **515**, 95 (2006).
- [22] M. R. Ramesh, S. Prakash, S. K. Nath, P. K. Sapra, B. Venkataraman, *Wear* **269**, 197 (2010).
- [23] T. Sundararajan, S. Kuroda, F. Abe, *Materials Transactions* **45**, 1299 (2004).
- [24] H. V. Hidalgo, F. J. B. Varela, A. C. Menéndez, S. P. Martínez, *Journal of Materials Science* **37**, 649 (2002).